Enhancement of Mechanical Properties in Non-Lethal Projectile Holders through High-Density Polyethylene and Alumina Nanocomposites

Noureddine Boumdouha[1,2,*], Jannick Duchet-Rumeau[1] and Jean-François Gerard[1]

[1]*UMR CNRS 5223 Ingénierie des Matériaux Polymères, Université de Lyon, INSA Lyon, 20, Avenue Albert Einstein, 69621 Villeurbanne, France*

[2]*Laboratoire Dynamique des Systèmes Mécaniques, École Militaire Polytechnique, BP17 Bordj El-Bahri, 16046 Algiers, Algeria*

Abstract:

This research looks into how to make and describe non-lethal projectile supports out of high-density polyethylene (HDPE) nanocomposites that are strengthened with alumina. This innovative approach enhances the material's mechanical properties and usability in security applications, significantly advancing over traditional materials. By integrating alumina nanoparticles, we improve the composite's strength and durability, which is critical for the reliability of non-lethal projectiles. Our findings contribute to materials science by providing a sustainable, efficient, and effective alternative for law enforcement and personal safety equipment.

*Corresponding Author
Tel: +213-697-005-578;
E-mail: boumdouhanoureddine@gmail.com

1. INTRODUCTION

In modern and creative applications, polymeric materials are advancing mainly in the aerospace, bicycles, products for consumers, agriculture, and sports industries [1]. Polymeric materials are essential materials science that will continue to grow in the following decades [2-4]. Recently, demand for polymer usage has significantly increased due to the growing world population and requirements [5]. Depending on the microstructure, polymers are shaped and connected with their mechanical properties [6]. That's how semicrystalline polymers get their tenacity to encounter the demands of products that endure difficult working situations (fatigue, impact, creep) [7]. For years, materials such as high-density polyethylene have received double attention [8] by depending heavily. They affect microstructure [9].

The widespread use of polyethylene in various applications, ranging from packaging materials to automotive components, underscores its significance in the modern world. However, the environmental implications of its extensive use and disposal have raised considerable concerns. Polyethylene, particularly in its high-density form (HDPE), poses challenges in waste management due to its non-biodegradable nature, leading to pollution and harm to marine life when not adequately recycled [10, 11]. To deal with these problems, our study looks into how HDPE can make non-lethal projectile supports. We want to combine the material's valuable qualities with environmental concerns by adding eco-friendly nanocomposites.

In the second half of the 1900s, polymers were strongly involved in processing. The goal was to develop and sell products that could substitute metals and other materials with robust mechanical properties. With the value of polymer products, it has become impossible to consider our world being rid of this material. Therefore, the creation and use of polymers have become a growth criterion [7]. Competition has long been undertaken to upgrade modern processes offering new grades and products. Polyethylene allows for generally simple formations such as extrusion or injection. It also has outstanding electrical insulation and shock absorption properties [12]. Annually, 500 billion to 1 trillion polythene bags are being used routinely worldwide, and on the coast, around 25 million tons of polymeric material are collected annually [13].

Polyethylene is the world's most advanced polymer, and everyone gets in touch with this polymer every day. At first, HDPE was considered an additional material commodity globally, although it was initially an insulator for electric cables. The strength of polyethylene today is due to its intrinsic properties, well-known usefulness, and extensive operating ability. Polyethylene can be manufactured as soft, flexible, durable, complex, and challenging. They can be seen in items of all sizes with a primary or intricate design. Among other things, HDPE is one of the most common engineering materials [14].

Modern petrochemical industries are rapidly expanding due to the low molecular weight of olefins like propylene, n-butene, and ethylene. The latter is the most important and most usable commodity in the petrochemical industry and is used in different materials. Composites have substantial advantages over conventional metal alloy materials. They have practical advantages: lightness, resistance to mechanical and chemicals, low maintenance, and freedom of shape. Their mechanical and chemical properties make it possible to extend the service life to improve protection from improved shock and fire resistance. They provide better thermal or sound insulation and good electrical insulation for some. They also improve design opportunities by enabling light structures and complex forms to perform multiple functions in each application sector. Filling material of 0.5 - 3 % by mass may have mechanical properties comparable to traditional composites, including 20 - 40 % [15].

Our second goal is to improve polymer compatibility with the filler, as using HDPE grafted onto maleic anhydride is appropriate. Maleic anhydride MA polyolefin graft is a significant branch of modified reactive polymers. MA-grafted polyethene HDPE is critical for its application as compatible polymer mixtures, adhesion promoters of polymers, composites, and binding agents for polymers and compounds. In the past two decades, the change in HDPE grafting by MA with molten organic peroxide has attracted attention [16].

Many studies have also shown that adequate coagents can reduce interlinkage, but the grafting degree has minimal effect. Adding coagents will also only marginally increase the grafting level [17]. Gaylord [18, 19] attempted to prevent the gel creation by adding certain electron-donating additives, notably dimethylacetamide and dimethyl sulfoxide, as well as three (nonylphenol) phosphates for high-density polyethylene and MA graft and got a coloured product

free of Gel. Gaylord [20], it was also reported that adding additives to the donor electron would reduce the degree of MAID grafting. Due to the secondary reactions in a grafted MA-HDPE, the two kinds of secondary reactions have the opposite effect on the molten reaction product viscosity.

In this study, we seek to make a holder for non-lethal projectiles where we add DCP peroxide to the level of mixtures of HDPE/carbon black and HDPE/alumina. The effect of HDPE on the degree of MA grafting and the melted viscosity of reactive materials is discussed. Supramolecular structures are formed spontaneously. The molecular chains are folded into lamellar crystals by a complex crystallization process, followed by lamellar crystal development into spherulites through radial growth. Mechanical characteristics like intensity and durability of semicrystalline polymer solids were responsible for structures [21, 22].

Secondary reactions are also followed by MA changing the polyolefin graft in the molten mass. HDPE is vulnerable to radical combination branching or crosslinking during grafting [23]. Therefore, this improvement is a function of the crosslinking system used in HDPE resin since certain features, like thermal stability and tensile strength, are reduced by peroxide-induced crosslinking [24]. Crosslinking of HDPE can be caused by adding peroxide [25]. But, optimizing production conditions is essential to ensure improved performance when mechanical, chemical, and thermal resistance is required. Much work has been done to refine the extruder's conditions and parameters to ease desired reactions while preventing adverse effects [20]. However, since radical reactions are fundamentally complex, the desired MA material is challenging to integrate without significant side reactions [17].

Composite materials offer significant advantages in developing non-lethal projectile supports, including enhanced lightweight properties, improved strength, and superior environmental resistance [26]. These characteristics are particularly beneficial as they produce safer, more efficient, and durable law enforcement tools. Integrating high-density polyethylene (HDPE) with alumina nanoparticles, for instance, reduces the projectile holders' overall weight and increases their resistance to wear and environmental degradation [27]. This innovative approach ensures that the materials used in non-lethal projectiles are effective in their application and aligned with sustainability goals [28].

However, the fabrication of HDPE/alumina nanocomposites poses some challenges, such as the dispersion of nanoparticles, the interfacial adhesion between the matrix and the filler, and the thermal stability of the polymer [29, 30]. Several techniques have been proposed to overcome these issues, such as melt blending, solution mixing, in situ polymerization, and thermokinetic mixing [29, 31]. Among these, thermokinetic mixing is an efficient and cost-effective method to produce HDPE/alumina nanocomposites with enhanced mechanical and thermal properties [32].

Creating the mixture's morphology during reactive compatibilization in the extruder is significant for the industry. The final morphology plays a crucial part in the final mixture properties. Also, for processability (blow moulding), the blends under shear are very significant and rely heavily on morphology. Developing knowledge of the relationship between formulation, morphology, and microstructure could lead to future improvements in product formulation and process characteristics [33]. Raman microscopy gives submicrometric chemical sensitivity to the imagery. The combination of Raman's and confocal microscopy permits the rejection of fuzzy Raman dispersion with less history output, 3D information, and better resolution. The distribution of alumina in a composite polyethylene matrix was investigated by Raman imaging [34]. Raman spectrum conversion into chemical imageries offers high difference and analysis reliability. Examining the picture approach enables a measurable evaluation of the mixing degree of the part that indicates where there is no partial intercalation.

The rapid evolution of material science has paved the way for significant advancements in non-lethal projectile technologies. Despite progress, challenges persist in optimizing the mechanical properties and durability of materials used in such applications. This study introduces a novel approach by incorporating alumina nanocomposites into HDPE, aiming to overcome these challenges and contribute to the field's advancement through innovative material solutions.

In response to the growing need for advancements in non-lethal law enforcement technologies, this study explores developing and characterizing non-lethal projectile holders fabricated from high-density polyethylene (HDPE) reinforced with alumina nanocomposites. Leveraging the unique properties of HDPE and the reinforcing capabilities of alumina

nanoparticles, this research aims to address current material limitations by enhancing mechanical strength and interface compatibility, which are crucial for the performance and reliability of non-lethal projectiles.

2. EXPERIMENTAL METHODS

2.1. Maleic Anhydride (MA)

Saidal offered the grafting of maleic anhydride ($C_4H_2O_3$), which has an ignition temperature of 70 °C. The auto-ignition temperature of the air is 376 °C. The minimum ignition rate for the air suspension is 50 g/m³. The maximum permissible concentration in the atmosphere of the working area is 1 mg/m³. With increased attention, the product may irritate the mucous membranes of the eyes and respiratory tract pathways. Despite its seriousness, it constitutes excellent support for the compressive properties of elongation and significantly increases the relative extension at breakage and fatigue endurance during repeated stretching. The polyurethane root interacts with a molecule of Maleic anhydride, which tends to bind to free radicals due to some reactions [35].

2.2. Liladox

Niax offered liladox is used as a source of free radicals in the polymerization of high-density polyethylene monomers. Its technical characteristics are a white laminar appearance and active oxygen of 2,69 wt. %, the density of 0.50 kg/l, and a melting point of 55 °C. This peroxide is heat-sensitive; these materials must be stored with strict temperature control measures. The risk of its explosion is also mitigated by mixing peroxide with an inert solid, where a stable temperature of less than 200 °C is the maximum transport temperature.

2.3. Perkadox

Niax offered perkadox, a flaky white powder containing technically pure, solid peroxydicarbonate used to treat unsaturated resins, an initiator of radical reactions at moderate temperatures. Mainly in the temperature range of 60 °C and above. Perkadox is a cyclo-aliphatic peroxydicarbonate used as an initiator in polymerizing monomers such as vinyl chloride and (methyl) acrylate. Its features are the peroxide content

of 95 % active oxygen, 3.81 %, a bulk density of 0.50 g/cm³, a melting point of 820 °C, a recommended storage temperature of less than 200 °C, a maximum transport temperature of 300 °C, and the stability of 6 months.

2.4. Benzoyl

Niax offered benzoyl peroxide, whose International Numbering System (INS) number is 928, and its molecular weight is 242.23. Melting point (degradable): 103-105 °C, density: 1.3 g/cm³. It is a colourless crystalline solid with a slight odour of benzaldehyde. It is a colourless liquid that is insoluble in water, partially soluble in alcohol, and slightly soluble in ether chloroform. One gram dissolves fully in 40 millilitres of carbon disulfide. Benzoyl peroxide, especially in dry areas, is a dangerous substance that is highly reactive and oxidizing and is known to combust spontaneously.

3. SAMPLE PREPARATION

3.1. Mixture's Preparation

Table **1** displays the most important basic compounds that contribute to preparing the optimal formulation for HDPE materials.

3.2. Physical-Chemical Tests

3.2.1. Fourier Transform Infrared Spectroscopy (FTIR)

Infrared spectroscopy research for HDPE using Perkin Elmer 1720 x Excalibur Series 3100 Diamond crystal ATR equipment operating at a variety of 3500 cm⁻¹-500 cm⁻¹ and 4 cm⁻¹ quality, and there were 100 scans. The specimens were taken using a powder in the KBr shell. Infrared spectrophotometry is a routine tool for polymer detection. We do not interpret the different spectrum bands directly but compare them with the reference spectrum for available products based on those characteristic bands that may have the sample spectrum to be defined. The scope of the product (HDPE with additives) and alloy ranges without and with compatibilizer were provided by all mixtures prepared between 0.5 and 3 %. The infrared spectrum of alloys is the sum of the component spectrums.

Table 1: Basic Compounds in the Preparation of HDPE

Mixture	HDPE_1	HDPE_2	HDPE_3	HDPE_4	HDPE_5	HDPE_6
Alumina (% by weight)	0.5	1	1.5	2	2.5	3

3.2.2. Raman Spectroscopy

The extruded HDPE Raman spectra were acquired with a confocal microscope WITEC, laser 532 nm, and 8 MW_10s at 10 Scans_x10 and collected at a room temperature of 0 cm^{-1} to 3500 cm^{-1} having a resolution in the spectral range of 3 cm^{-1}. Everyone's Raman absorption spectra have been smoothed with the polynomial order 5 Savitzky method, window points 10 [36] and normalized in Origin 2018.

In the past two decades, polyethylene has been commonly used for Raman spectroscopy, and the properties of Raman's major bands are well set up (Table **2**). Standard internal modes of 1000 to 16 000 cm^{-1} are widely used for morphological structure studies, and three vibratory zones can be separated [37, 38]:

- C=C at 1000 to 1200 cm^{-1}, molecular orientation prone, stresses, and conformity.

- CH$_2$ folding modes amid 1400 and 1470 cm^{-1} chain-settling sensitive.

- CH$_2$ torque vibrations of approximately 1295 cm^{-1} will be used as a standard solution.

Community theory implementation in the modes of vibration predicts crystalline polyethylene. The simple beat is divided by the two polyethylene chains per unit mesh into two components of different symmetry [36]. The effect is called the factor group division [36, 39, 40]; Raman divides bending vibration -CH$_2$- between 1415 cm^{-1} and 1440 cm^{-1} bands Raman. The strip is thus considered a direct measurement of material crystallinity and is used by Hagedorn and Strobl to test the structural phases [41].

3.3. Microstructural Characterization

3.3.1. Optical Microscope

Light microscopy helps to assess the structure and characteristics of the HDPE mixture to estimate the effect of the various alumina levels on the morphology. The microscopic study of polymers allows the micro and nonstructural features of the HDPE mix to be analyzed and characterized. Light microscopic magnification can be used to gain chemical and physical details about the structural properties of the HDPE mixture. Polymers, conversely, form crystalline or amorphous structures in part. Partially crystalline polymers are anisotropic optically [45]. Polarization is also the most common process for the analysis of polymers [46].

4. RESULTS

4.1. HDPE Mixture Evaluation

4.1.1. Adding Compatibility

There are many issues with synthesizing a nanocomposite material of a polyethylene matrix and an alumina filler, primarily because the non-polar matrix is not miscible with the polar alumina reinforcement. The melt formation of the matrix polymer one, where polar or polarized functional chemical groups are randomly inserted or grafted along the polymer chain, seems successful. The proportions of grafted polar groups differ between 0.5 and 3 mol %, which are appropriate for promoting the miscibility of polymer clay. We, therefore, performed a maleic anhydride HDPE transplant. But for the correct peroxide option, we employed three types of lilacs, paradox and benzoyl peroxide to prepare the mixtures, which summarize the

Table 2: Basic Vibrations of Interest in Semicrystalline Polyethylene [42, 43]

Vibrations	Amount of wave (cm^{-1})	Symmetry form
First-order LAM	5–30	A$_g$
Asymmetric C–C bond stretching vibration	1060 (Crystalline phase)[a] and 1080 (amorphous phase)	B$_{2g}$ + B$_{3g}$
Symmetric C–C bond stretching vibration	1130 (Crystalline phase)[a]	A$_g$[b] + B$_{1g}$
Distortion of the vibration CH$_2$	1295 (Crystal phase)[a] and 1305 (Step amorphous)	B$_{2g}$ + B$_{3g}$
The resonance of Fermi CH$_2$ and the primary CH$_2$ rocking vibration overtone	1415 (Orthorhombic crystal) and 1440 and 1460	A$_g$

[a]It is assumed that as well as the pure crystallized material, the presence of many subsequent chain transformation conformations could also explain the strength of these crystal bands. Therefore, these bands are sensitive to fractions of all-trans molecules in this study [44].
[b]Only Ag-type symmetry was observed unequivocally in a Raman spectrum for the 1130 cm^{-1} Raman band.

proportions of each critical component of the formulations in Table **3**:

Table 3: **An Overview of the Compatibilizers Used for the Peroxide Selection Analysis**

Mixture	HDPE	Peroxide	MA
1	96 %	1 % of Liladox	3 %
2	96 %	1 % of Perkadox	3 %
3	96 %	1 % of Benzoyl	3 %

The grafting reaction was conducted with a two-screw HaLake Record RC90. Maleic anhydride MA and peroxide DCP were absorbed in acetone and combined with HDPE pellets before extrusion. Following acetone volatilization, MA and DCP adhered reliably to the pellets. The extruder's temperature profiles, 140 °C and 160 °C 180 °C and 200 °C were reached, and its velocity was 60 rpm. After refreshing in a bath, the extruded strips have been cut into pellets about 4 mm long. To extract maleic anhydride and free peroxides, we have cleaned up our product of approximately 3 g of the substance in 100 ml of toluene xylene by reflux heating. The whole thing was precipitated in a continuous 500 ml acetone and then vacuum filtered. Wash with acetone three times to remove the unbranched maleic anhydride and peroxides. Vacuum drying lasts 12 hours for the evaporation of acetone. The product of the grafting process was purified by precipitation and then used to calculate the grafting grade. Around 3 g of the substance was dissolved in 100 ml of xylene reflux, and in 500 ml of acetone, the solution was continually precipitated.

4.1.2. Infrared Grafting Rate Determination

Thin plates were prepared for the passage of our samples in Infrared via the press. The ratio of the area with characteristic carbonyl peaks at 1790 cm^{-1} of the maleic anhydride group to 3000 cm^{-1} of the polyethylene class is measured from the infrared spectrum of the three mixtures. The ratio of these noted X peaks would show the relative percentage of each species (5).

$$X = \frac{Carbonyl\ group\ peak\ area\ 1790\ cm^{-1}}{Methyl\ group\ peak\ area\ 3000\ cm^{-1}} \qquad (5)$$

Compared with pure HDPE, we observed carbonyl groups peaking at 1970 cm^{-1}, suggesting the grafting reaction of maleic anhydride. Furthermore, the absorption of these peaks differs from one wavelength to another since the grafting rate was determined as follows:

Mixture n ° 1 (Perkadox peroxide):

$$X1 = \frac{3.55\ A\ cm^{-1}}{581.97\ A\ cm^{-1}} = 0.006099 = 0.61\%$$

Mixture n ° 2 (Liladox peroxide):

$$X2 = \frac{1.93\ A\ cm^{-1}}{515.69\ A\ cm^{-1}} = 0.00375 = 0.37\%$$

Mixture n ° 3 (Benzoyl peroxide):

$$X3 = \frac{5.37\ A\ cm^{-1}}{507.17\ A\ cm^{-1}} = 0.01058 = 1.09\%$$

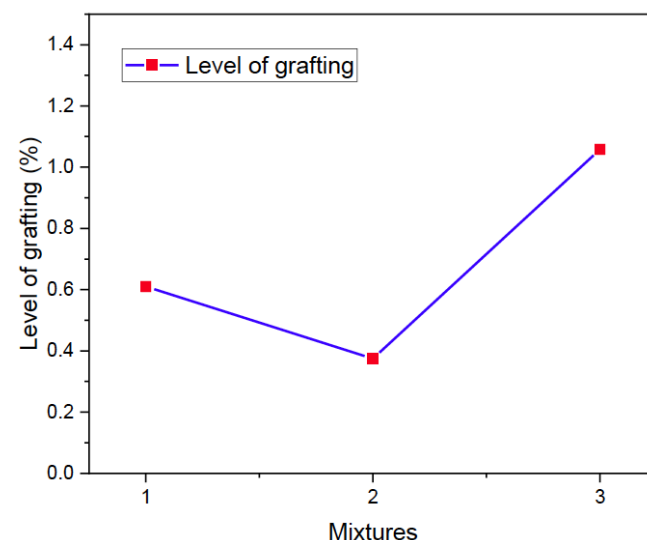It is evident from this figure that with Benzoyl Peroxide, the best grafting rate is obtained (Figure **1**).

Figure 1: Variability in the rate of mixture grafting.

The stress cracking test results are presented in Table **4**.

Table 4: **Results for Stress Cracking Mixtures**

Mixture	The specimens' fractional time (hour)
1	16
2	21
3	26

The resistance to slow cracking on a surfactant medium decreases considerably, likely because of the small percentage of the compatibility agent. The best

results are seen for mixtures containing (2.5 % - 2.5 %) HDPE/CB percentage, HDPE/Alumina, and Mixture 3.

4.2. Results of the Protocol for Grafting

4.2.1. Fourier Transform Infrared Spectroscopy (FTIR)

Before starting the HDPE analysis, the spectroscopic characteristics of the sample must be known in its pure state and after the incorporation of additives. The latter is used as a guide in our HDPE development analysis. Virgin HDPE polyethylene is composed of ethylene CH_2 groups, and their IR spectrum contains high medium and low-intensity CH_2 groups, which have wavelengths collected in Table **5** [47]. FTIR analysis checks for maleic anhydride grafting into the HDPE-MA formation chain. The latter is used as a mixture compatibilizer.

Table 5: Main Vibrations of Pure HDPE

Wave number (cm^{-1})	Attribution
2917	Asymmetric elongation C-H
2848	Symmetrical elongation C-H
1472	CH_2 strain in the plane (shear)
1465	CH_2 strain in-plane (rotation)
730	CH_2 strain (rotation)
720	CH_2 deformation out of a plane (sway)

The cleaned products were moulded in approximately 0.05 mm thick compression films for Fourier infrared spectroscopy FTIR characterizations. In all samples, the characteristic peaks of aliphatic hydrocarbons (–CH_3 and –CH_2), considered the polyethylene reference, are found between 2848 and 2917 cm-1. As shown in Figure **2**, the opposite:

HDPE and HDPE/CB and HDPE/Alumina mixtures. Compared with the grafted HDPE and MA spectrums, the MA grafted HDPE mixture spectra had the saturated cyclic anhydride characteristic. The 1862 cm^{-1} and 1785 cm^{-1} bands were produced by symmetrical and asymmetrical C = O stretch modes. The 1711 cm^{-1} bands represent C=O Maleic acid. The standard MA-grafted HDPE mixture bands ranged from the HDPE 1 % peroxide and 1 % liladox to the 1 % benzoyl peroxide, according to Table **6**.

The bands at 1862 cm^{-1} and 1785 cm^{-1} were symmetrically and asymmetrically stretched with C = O. The 1711 cm^{-1} bands are a component of maleic anhydride's C=O [48]. The table shows the characteristic bands of the grafted MA and HDPE

mixture. They indicated that both HDPE mixtures had been grafted with MA.
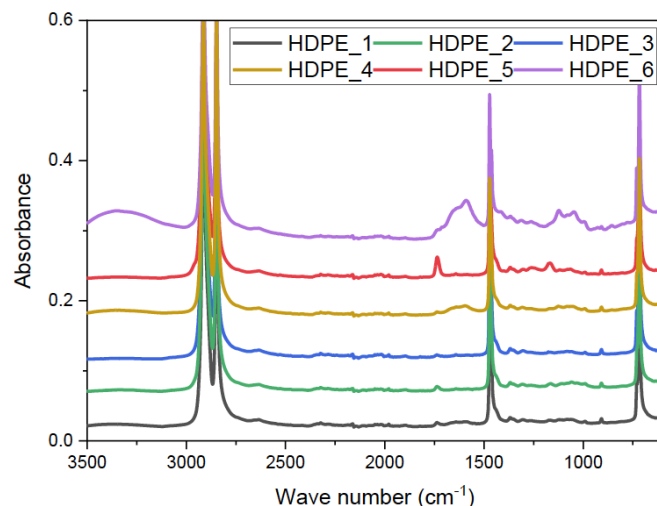

Figure 2: Fourier infrared spectroscopy of HDPE, HDPE/CB 2 %, HDPE/Alumina 2.5 %, and MA grafted products: mixture 01, mixture 02, and mixture 03.

4.2.2. Differential Scanning Calorimetry (DSC)

However, adding MA particles affects the crystallization temperature of mixtures 1, 2, and 3, which is consistent with Luljeta Raka *et al*. [49].

4.2.3. Raman Spectroscopy

The Raman spectrums of the treated samples reflect all the compositions in HDPE/Alumina mixtures (0.5 % - 3 % by weight) and Raman polymer chains of polyethylene displacements (Table **7**). In short, 1063, 1132, and 1296 cm^{-1} offsets are obtained from the C=C stretch and the -CH_2- torque. The average Raman change of 1445 cm^{-1} is correlated with three vibration modes (CH_2) of the crystalline HDPE (one vibration mode and two vibrational modes scissors) [50]. The heavy Raman offset at 2845 cm^{-1} and 2883 cm^{-1} results in asymmetrical and symmetrical deformation of the CH_2 units, respectively [51, 52]. Table **7** introduces the ideal HDPE mixture predictive models.

Figure **3** shows a typical composite spectrum Raman HDPE of the HDPE/Alumina composites by weight % HDPE mixture. In Raman images, the traditional Raman bands are used to differentiate these components. The alumina Raman spectrum is absent in the HDPE pure, namely 2000 ~ 2500 cm^{-1} centre-band, consistent with stretches of the CO ring and the COC stretch modes between chains [53]. Adding testing of alumina results of 2000 ~ 2500 cm^{-1} bands allocated to the skeletal bending modes, including CC and CO skinny stretch modes.

Table 6:   Principal Infrared Absorption Bands of HDPE and MA-Grafted

	Mixture	C=O	C=O of MA
HDPE_1	HDPE	1785	-
HDPE_2	HDPE/CB 2 %	1785	-
HDPE_3	HDPE/Alumina 2.5 %	1784	-
HDPE_4	HDPE 96 %/ Liladox 1 %/ MA 3 %	1862	1712
HDPE_5	HDPE 96 %/ Perkadox 1 % /MA 3 %	1864	1711
HDPE_6	HDPE 96 %/ Benzoyl 1 %/ MA 3 %	1865	1711

Table 7:   Main HDPE Raman Changes

The shift of Raman (cm^{-1})	Bond	Mode of vibration	Step Phase	Raman tensor
1063 1132 1296	-C-C- -CH$_2$-	Extend and twist	Anisotropic and crystalline areas	$B_{2g} + B_{3g}$
1445	-CH$_2$-	One mode and two-mode of scissoring	Crystalline (orthorhombic)	A_g
2883	-CH$_2$-	Symmetrical extension	Crystalline and amorphous	-
2845	-CH$_2$-	Asymmetric extension	Crystalline and amorphous	-

The spectrum of the Raman has specific bands, including a tight band at 1296 cm^{-1}, which corresponds to the CH$_2$ crystalline phase torsion types [54]. Also, the Raman bands with CC stretch modes of 1063 and 1132 cm^{-1} in the crystalline and anisotropic polyethylene phases are used for the research [54].

In the chemical pictures, the HDPE system areas dominate. The Raman spectrum of polyethylene is close to melting pure HDPE. The two green colours represent the regions containing alumina in the chemical images. The blue area on the chemical maps is more prominent in HDPE. The Raman spectrum refers to the mixture field that has characteristic Raman bands. These areas (blue) show a potent component mix. Chemical imaging can also differentiate the regions in which loads and loads and matrix are closely interacting. They offer the presence of two antagonistic mechanisms: the aggregation phase and the mixing process. The Raman images of HDPE/Alumina composites are illustrated in Figure **4**.

The transparent areas in Figure **4** display the strong band of Raman 2250 cm^{-1} high and confirm the existence of alumina in the mapped region. The blue colour shows the part where the bands of Raman picked are not present or where their strength is inferior, although the hue of the bands matches the maximum severity. Alumina forms islets in a polyethylene matrix consistent with scanning microscopic images, suggesting significant aggregation. The forms of these islands are circular and irregular. Raman images indicate that the charges of alumina are not distributed through the volume of polyethylene but combined with the matrix polyethylene. The strength of the selected Raman bands at the image level also represents the surface morphology for the composite portion. Images showing the intensity of the Raman ribbon-based about 1132 cm^{-1} show the surface characteristics of the cutting path. A lower ribbon intensity of ~ 1296 cm^{-1} of dark brown is the presence of alumina aggregates and voids.

Alumina seems to have a greater propensity to agglomerate during polyethylene melting. On the other hand, sand grains for the compaction method may remain intact and are derived from the industrial drying process. In preparing nanocomposites of high quality, this effect is not desirable. Furthermore, the alumina accumulation reduces the surface area observed, preventing Raman and chemical pictures from assessing the stoichiometric component ratio. Instead, mixing the degree between load and performance in the matrix of this method is only helpful for quantifying. Alumina seems to blend with HDPE to a greater degree.
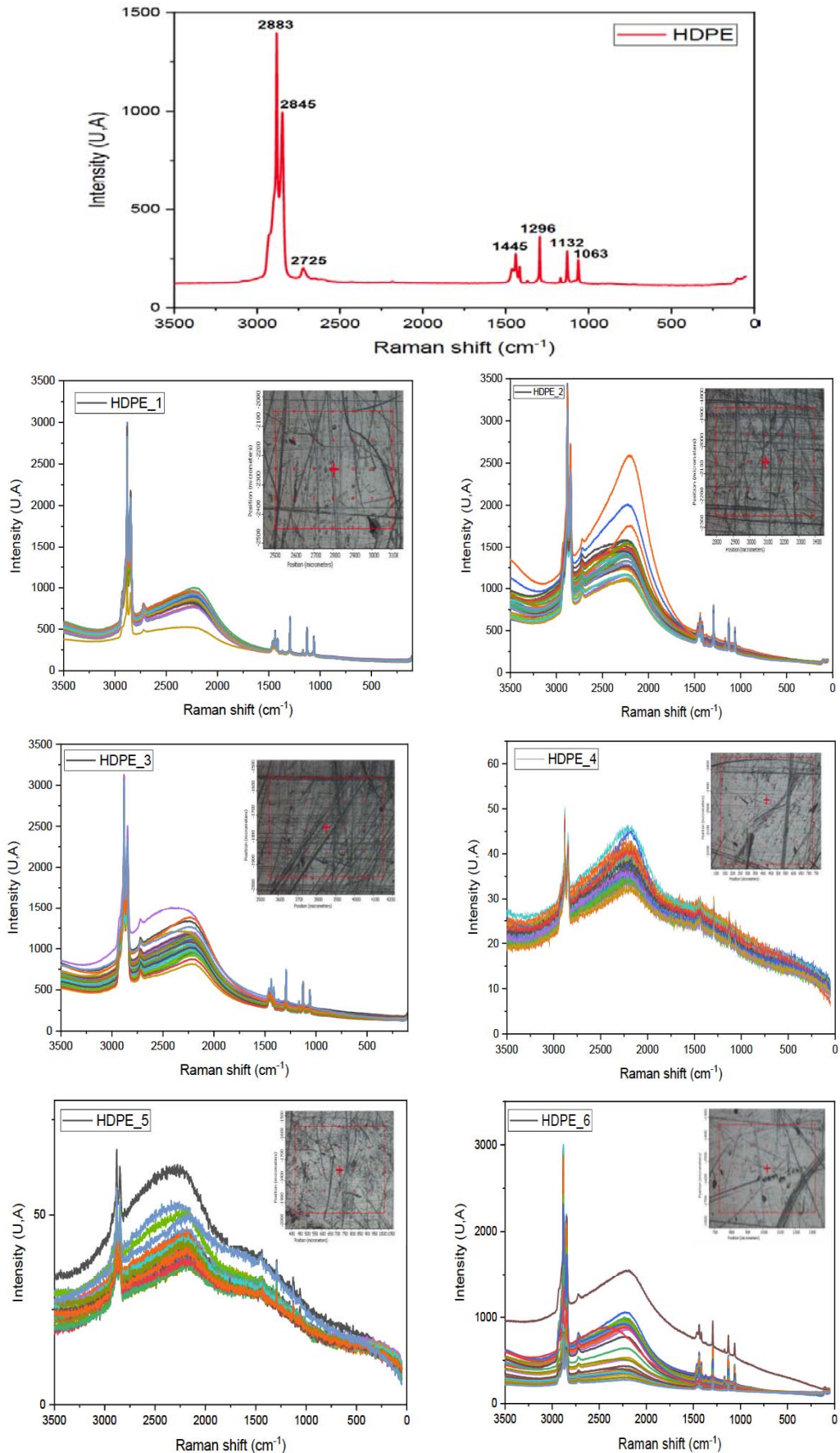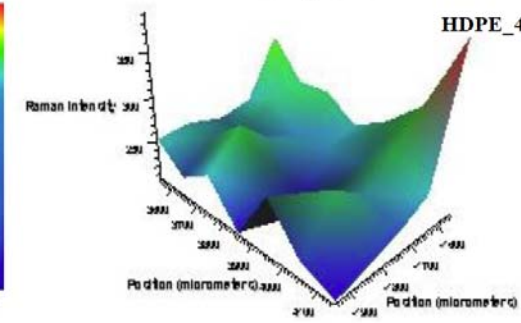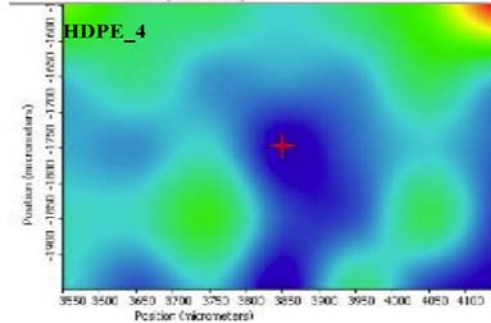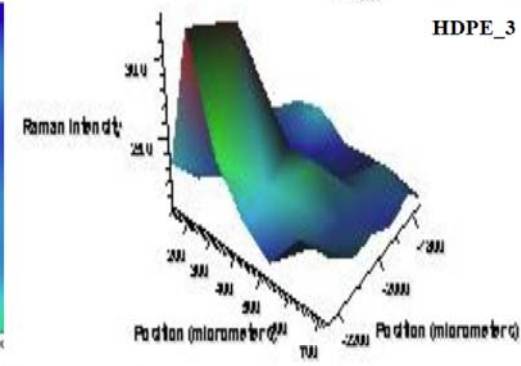
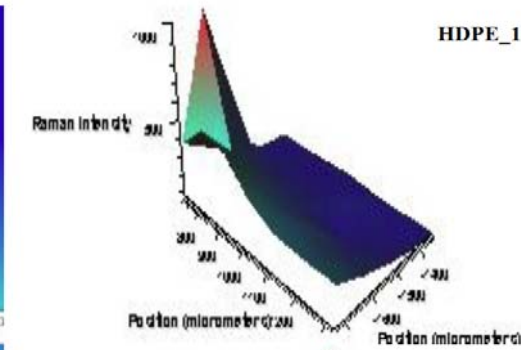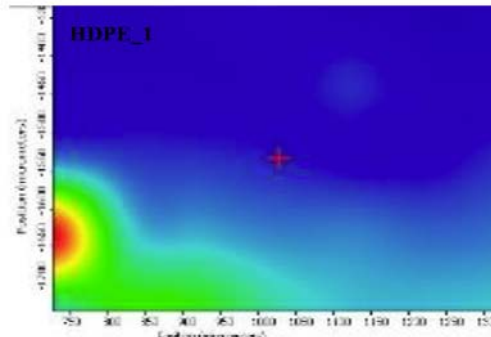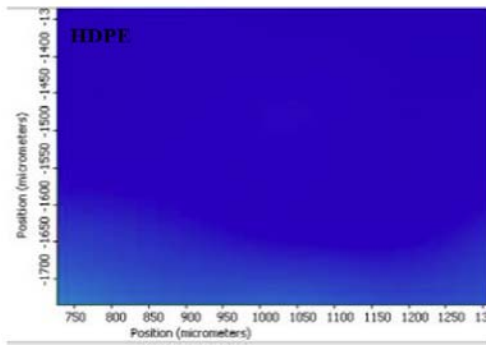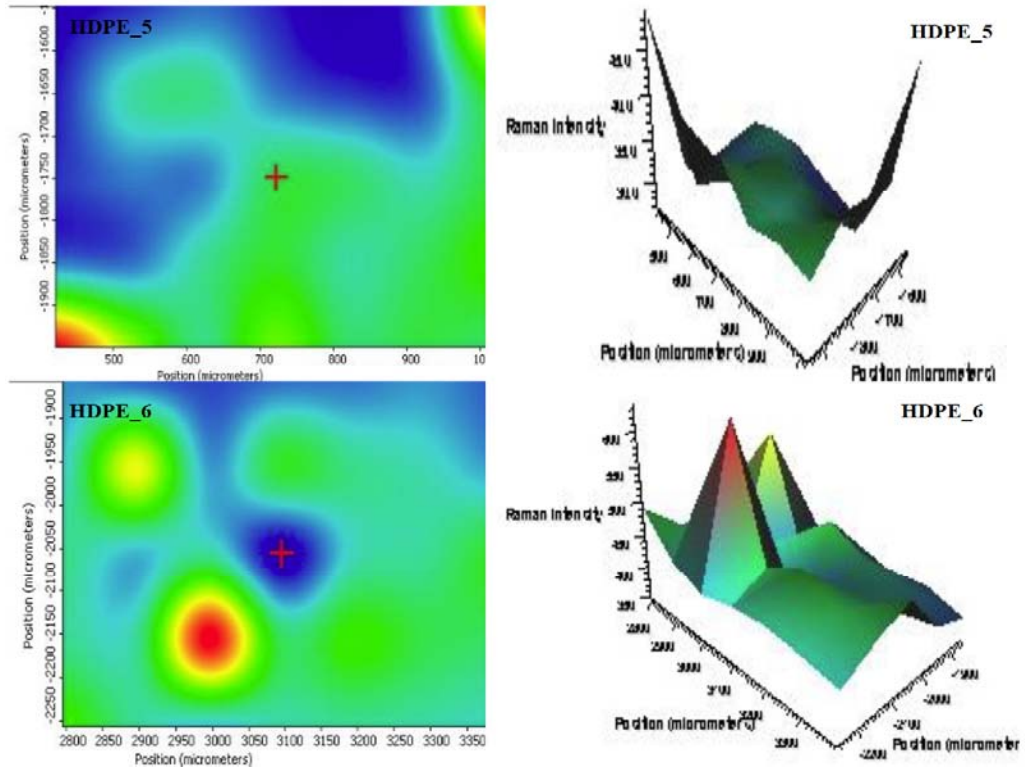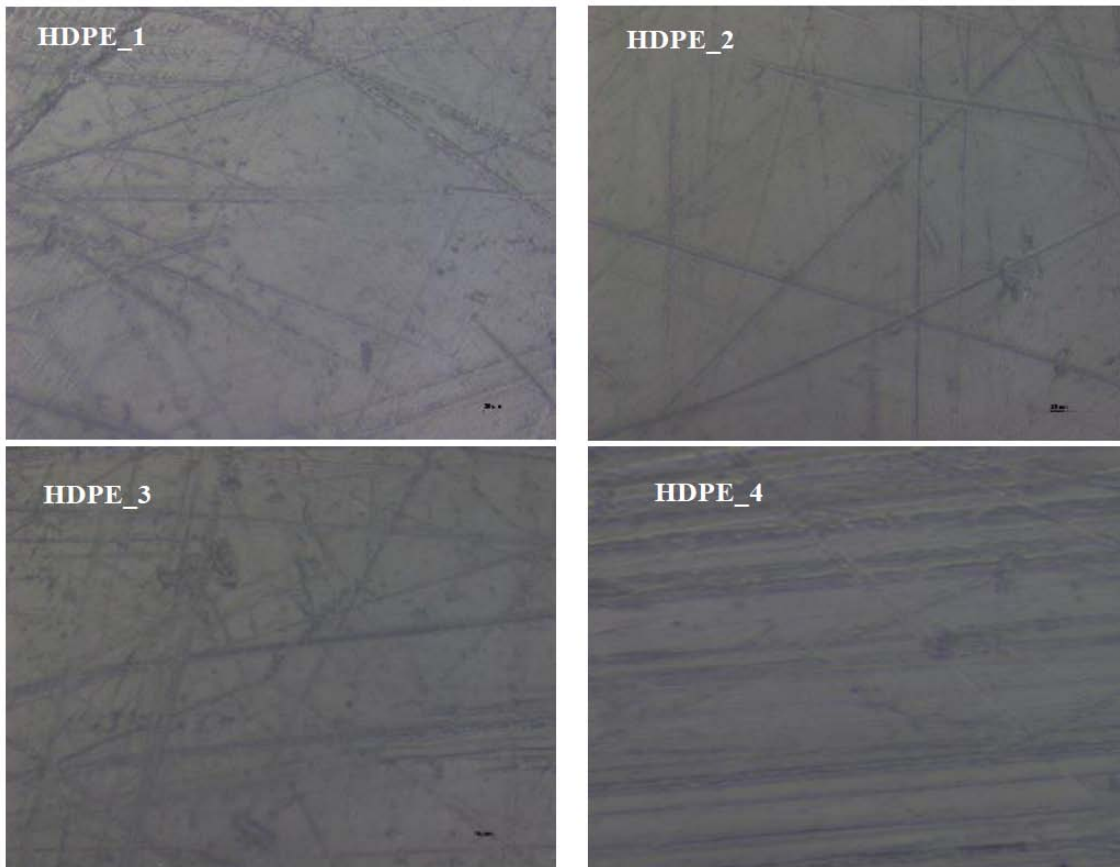**Figure 3:** Typical composite spectrum Raman HDPE.
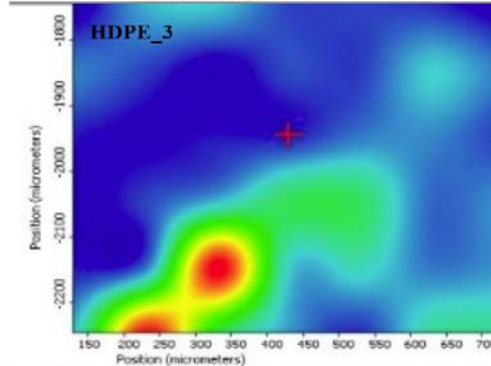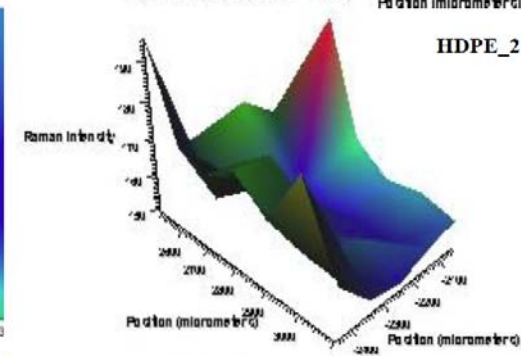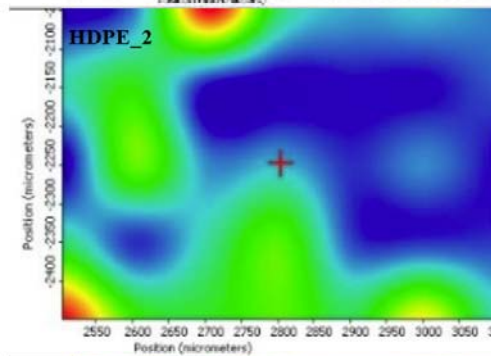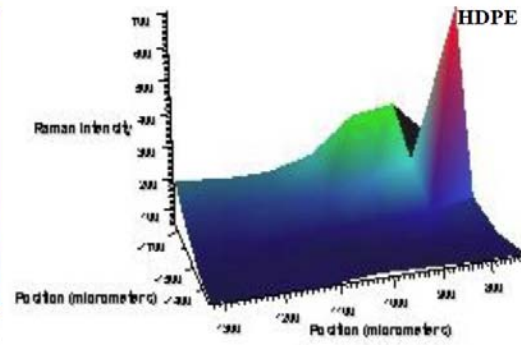
Figure 4: Typical Raman images of alumina/HDPE composites demonstrating Raman band strength.
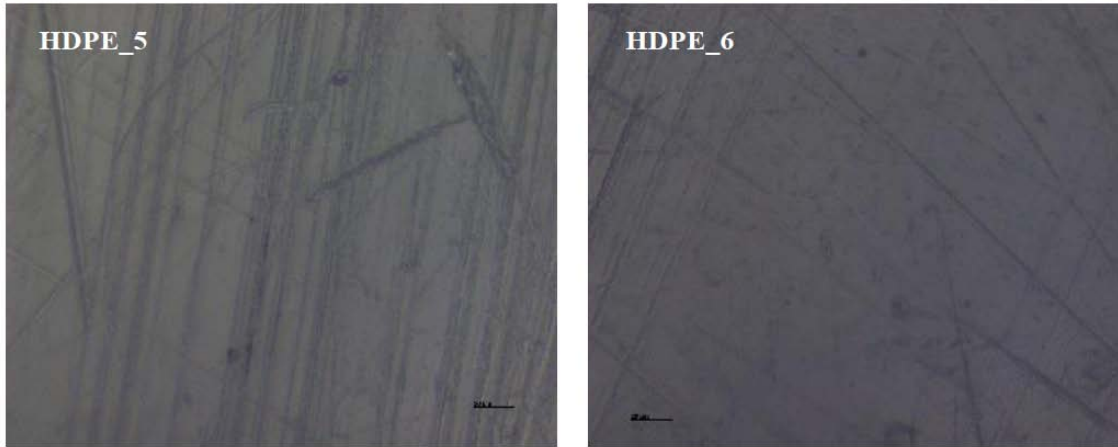
(Figure 5). Continued.

Figure 5: HDPE surfaces Optical microscopy images.

4.3. Microstructural Characterization

4.3.1. Optical Microscope

The pictures for optical microscopy in Figure **5** demonstrate the macroscopic dispersion of the alumina nanopowder at the macroscopic level in the injection-moulded samples. The HDPE reference shows a consistent morphology where crystalline superstructures are not visible, as the limits of the spherulites in the photos. Due to the alumina nanoparticles scattered at the submicron level, the HDPE sample is very dark. However, much alumina powder is agglomerated into many or tens of microns.

The HDPE_6 sample has excellent alumina dispersion and few visible characteristics, such as gel particles. Whatever the insert surface type, the HDPE_6 is heterogeneous to the HDPE_5 surface. The polymeric objects, HDPE_3 and HDPE_4, are very similar. The HDPE_1 and HDPE_2 contain surface scratches but retain the optical luminosity (observed by the naked eye). They may be because of the slightly improved ruggedness offered by alumina inserts and the crystalline nature of alumina. The samples injected with the insert of 0.5 % were still very clean, but the HDPE sample surface became heterogeneous as the number of injections increased.

This research looked at the mechanical properties of HDPE mixed with alumina nanocomposites. Specifically, we looked at its tensile strength, resistance to impact, and modulus of elasticity. Including alumina nanoparticles significantly improved the material's mechanical performance, which is crucial for the durability and reliability of non-lethal projectile holders. It is important to note that, as electron microscopy demonstrated, the HDPE matrix and alumina nanoparticles stuck together better, allowing improvements. These results indicate that alumina-reinforced HDPE nanocomposites could be helpful in advanced engineering tasks, providing a promising answer to the problems that current materials have.

5. CONCLUSIONS

The study presents a significant advancement in materials science, particularly in developing sustainable and efficient materials for non-lethal security applications. Our research shows that adding alumina nanoparticles to HDPE matrices greatly enhances their mechanical properties, including tensile strength and impact resistance. These are important for making projectile supports that do not kill. This improves the performance and reliability of security devices and promotes environmental sustainability through the potential for recycling and reduced environmental impact. Furthermore, the compatibility of alumina with HDPE highlights the feasibility of creating advanced nanocomposites with tailored properties for specific applications. These contributions are expected to pave the way for further research in nanocomposite materials, offering innovative solutions for law enforcement and personal safety equipment.

CONFLICTS OF INTEREST

The authors note that the investigation was carried out without any corporate or financial arrangement, which could be perceived as a conflict.

ACKNOWLEDGEMENTS

out this work through the availability of the DRFPG executives and the means at our disposal. Polymed Skikda made our first contact with the petrochemical industry world. I thank Professor Jean-François Gerard and Professor Jannick Duchet-Rumeau for allowing me to work within the Laboratory of Polymer Materials Engineering, UMR 5223 CNRS/INSA Lyon. The IMP laboratory offered me an ideal working environment during these internship periods.

AUTHOR CONTRIBUTIONS

Boumdouha Noureddine: Formal analysis, Writing - Original Draft Preparation, Funding acquisition, Resources, Writing - Review and Editing, Software, Investigation. Duchet-Rumeau Jannick: Data Curation Conceptualization and methodology. Gerard Jean-François: Review & Editing, Project administration, Supervision, visualization. All writers approved the final manuscript.

REFERENCES

[1] Boumdouha N, Safidine Z, Boudiaf A, Duchet-Rumeau J, Gerard J-F. Experimental study of the dynamic behaviour of loaded polyurethane foam free fall investigation and evaluation of microstructure. Int J Adv Manuf Technol 2022.
https://doi.org/10.21203/rs.3.rs-792400/v1

[2] Gurunathan T, Rao CRK, Narayan R, Raju KVSN. Polyurethane conductive blends and composites: Synthesis and applications perspective. J Mater Sci 2013; 48(1): 67-80.
https://doi.org/10.1007/s10853-012-6658-x

[3] Szleifer I, Yerushalmi-Rozen R. Polymers and carbon nanotubes - Dimensionality, interactions and nanotechnology. Polymer (Guildf)., SPEC. ISS. 2005; 46(19): 7803-7818.
https://doi.org/10.1016/j.polymer.2005.05.104

[4] Svensson A, Hasselström J. Fundamental physical testing of rattle-Design and evaluation of a rattle producing test rig 2017.

[5] Curlee TR, Das S. Plastic wastes: management, control, recycling, and disposal. Noyes Pubns 1991; 201.

[6] Boumdouha N, Safidine Z, Boudiaf A, Oukara A, Tria DE, Louar A. Mechanical and microstructural characterization of polyurethane foams. in 8th Chemistry days JCh8-EMP, Bordj El Bahri, Algeria: Military Polytechnic School (EMP) 2019; p. 169.

[7] Boumdouha N, Safidine Z, Boudiaf A. Experimental Study of Loaded Foams During Free Fall Investigation and Evaluation of Microstructure. Int J Adv Manuf Technol 2021.
https://doi.org/10.21203/rs.3.rs-792400/v1

[8] Addiego F. Caractérisation de la variation volumique du polyéthylène au cours de la déformation plastique en traction et en fluage. Institut National Polytechnique de Lorraine 2006.

[9] Baïlon J-P, Dorlot J-M. Des matériaux. Presses inter Polytechnique 2000.

[10] Xu G, Wang Q. Chemically recyclable polymer materials: polymerization and depolymerization cycles. Green Chem 2022; 24(6): 2321-2346.
https://doi.org/10.1039/D1GC03901F

[11] Koshti R, Mehta L, Samarth N. Biological Recycling of Polyethylene Terephthalate: A Mini-Review. J Polym Environ 2018; 26(8): 3520-3529.
https://doi.org/10.1007/s10924-018-1214-7

[12] Boumdouha N, Louar MA. Influence of Microstructure on the Dynamic Behaviour of Polyurethane Foam with Various Densities. J Basic Appl Sci 2023; 19: 131-150.
https://doi.org/10.29169/1927-5129.2023.19.12

[13] Sangale MK. A Review on Biodegradation of Polythene: The Microbial Approach. J Bioremediation Biodegrad 2012; 03(10): 164-172.
https://doi.org/10.4172/2155-6199.1000164

[14] Chen J, *et al*. Surface modification of ion implanted ultra high molecular weight polyethylene. Nucl Instruments Methods Phys Res Sect B Beam Interact with Mater Atoms 2000; 169(1-4): 26-30.
https://doi.org/10.1016/S0168-583X(00)00011-2

[15] Bureau MN, Di Francesco E, Denault J, Dickson JI. Mechanical behavior of injection-molded polystyrene/polyethylene blends: fracture toughness vs. fatigue crack propagation. Polym Eng Sci 1999; 39(6): 1119-1129.
https://doi.org/10.1002/pen.11499

[16] Li C, Zhang Y, Zhang Y. Melt grafting of maleic anhydride onto low-density polyethylene/polypropylene blends. Polym Test 2003; 22(2): 191-195.
https://doi.org/10.1016/S0142-9418(02)00079-X

[17] Lu B, Chung TC. Synthesis of maleic anhydride grafted polyethylene and polypropylene, with controlled molecular structures. J Polym Sci Part A Polym Chem 2000; 38(8): 1337-1343.
https://doi.org/10.1002/(SICI)1099-0518(20000415)38:8<1337::AID-POLA18>3.0.CO;2-8

[18] Gaylord NG, Mehta R. Peroxide-catalyzed grafting of maleic anhydride onto molten polyethylene in the presence of polar organic compounds. J Polym Sci Part A Polym Chem 1988; 26(4): 1189-1198.
https://doi.org/10.1002/pola.1988.080260419

[19] Gaylord NG, Mehta R, Kumar V, Tazi M. High density polyethylene-g-maleic anhydride preparation in presence of electron donors. J Appl Polym Sci 1989; 38(2): 359-371.
https://doi.org/10.1002/app.1989.070380217

[20] Gaylord NG, Mehta R, Mohan DR, Kumar V. Maleation of linear low-density polyethylene by reactive processing. J Appl Polym Sci 1992; 44(11): 1941-1949.
https://doi.org/10.1002/app.1992.070441109

[21] Rao N, O'Brien K. Mechanical Properties of Solid Polymers. John Wiley & Sons 1998.
https://doi.org/10.3139/9783446402447.001

[22] Boumdouha N, Safidine Z, Boudiaf A, Oukara A, Tria DE, Louar MA. Manufacture of polyurethane foam with a certain density. in The International Conference on Recent Advances in Robotics and Automation ICRARE'18, Monastir - Tunisia: CES International Joint Conferences 2018; pp. 21-30.

[23] Linul E, Marşavina L, Vălean C, Bănică R. Static and dynamic mode I fracture toughness of rigid PUR foams under room and cryogenic temperatures. Eng Fract Mech 2020; 225: 106274.
https://doi.org/10.1016/j.engfracmech.2018.12.007

[24] Khonakdar HA, Morshedian J, Wagenknecht U, Jafari SH. An investigation of chemical crosslinking effect on properties of high-density polyethylene. Polymer (Guildf) 2003; 44(15): 4301-4309.
https://doi.org/10.1016/S0032-3861(03)00363-X

[25] Sultan BA, Palmlof M. Advances in crosslinking technology. Plast. Rubber Compos. Process Appl 1994; 21(2): 65-73.

[26] Boumdouha N, Duchet-Rumeau J, Gerard J-F, Tria DE, Oukara A. Research on the Dynamic Response Properties of

Nonlethal Projectiles for Injury Risk Assessment. ACS Omega 2022; 7(50): 47129-47147.
https://doi.org/10.1021/acsomega.2c06265

[27] Costa ILM, Zanini NC, Mulinari DR. Thermal and Mechanical Properties of HDPE Reinforced with Al2O3 Nanoparticles Processed by Thermokinectic Mixer. J Inorg Organomet Polym Mater 2021; 31(1): 220-228.
https://doi.org/10.1007/s10904-020-01709-0

[28] Boumdouha N, Safidine Z, Boudiaf A. Preparation of Nonlethal Projectiles by Polyurethane Foam with the Dynamic and Microscopic Characterization for Risk Assessment and Management. ACS Omega 7(18): 16211-16221.
https://doi.org/10.1021/acsomega.2c01736

[29] Chen G, Hong Zhang X, Liang Qiao J. Effect of nano-fillers on conductivity of polyethylene/low melting point metal alloy composites. Chinese J Polym Sci English Ed. 2015; 33(3): 371-375.
https://doi.org/10.1007/s10118-015-1589-z

[30] Chee CY, Song NL, Abdullah LC, Choong TSY, Ibrahim A, Chantara TR. Characterization of mechanical properties: Low-density polyethylene nanocomposite using nanoalumina particle as filler. J Nanomater 2012; 2012.
https://doi.org/10.1155/2012/215978

[31] Khan WU, Bahar MK, Mazhar H, Shehzad F, Al-Harthi MA. Recent advances in nitride-filled polyethylene nanocomposites. Adv Compos Hybrid Mater 2023; 6(6): 1-27.
https://doi.org/10.1007/s42114-023-00802-5

[32] Ramesh M, Rajeshkumar LN, Srinivasan N, Kumar DV, Balaji D. Influence of filler material on properties of fiber-reinforced polymer composites: A review. E-Polymers 2022; 22(1): 898-916.
https://doi.org/10.1515/epoly-2022-0080

[33] Boumdouha N. Project Polytechnique Reporting. Lyon, French 2022.

[34] Cosby T, Aiello A, Durkin DP, Trulove PC. Kinetics of ionic liquid-facilitated cellulose decrystallization by Raman spectral mapping. Cellulose 2021; 28(3): 1321-1330.
https://doi.org/10.1007/s10570-020-03643-3

[35] Boumdouha N, Safidine Z, Boudiaf A. A new study of dynamic mechanical analysis and the microstructure of polyurethanefoams filled. Turkish J Chem 2022; 46(3): 814-834.
https://doi.org/10.55730/1300-0527.3371

[36] Kravitz LC, Kingsley JD, Elkin EL. Raman and infrared studies of coupled PO4-3 vibrations. J Chem Phys 1968; 49(10): 4571-4575.
https://doi.org/10.1063/1.1669918

[37] Snyder RG, Schachtschneider JH. Vibrational analysis of the n-paraffins-I. Assignments of infrared bands in the spectra of C3H8 through n-C19H40. Spectrochim Acta 1963; 19(1): 85-116.
https://doi.org/10.1016/0371-1951(63)80095-8

[38] Pezzotti G. Raman spectroscopy of biomedical polyethylenes. Acta Biomater 2017; 55: 28-99.
https://doi.org/10.1016/j.actbio.2017.03.015

[39] Ishii K, Nukaga M, Hibino Y, Hagiwara S, Nakayama H. Infrared and Raman Studies of Structural Relaxation in Amorphous Tetracosane, n -C 24 H 50. Bull Chem Soc Jpn 1995; 68(5): 1323-1330.
https://doi.org/10.1246/bcsj.68.1323

[40] Williams Q, Knittle E. Infrared and raman spectra of Ca5(PO4)3F2-fluorapatite at high pressures: Compression-induced changes in phosphate site and Davydov splittings. J Phys Chem Solids 1996; 57(4): 417-422.
https://doi.org/10.1016/0022-3697(95)00285-3

[41] Strobl GR, Hagedorn W. Raman Spectroscopic Method for Determining the Crystallinity of Polyethylene. AIP Conf Proc 1978; 16(7): 1181-1193.
https://doi.org/10.1002/pol.1978.180160704

[42] Gall MJ, Hendra PJ, Peacock OJ, Cudby MEA, Willis HA. The laser-Raman spectrum of polyethylene. The assignment of the spectrum to fundamental modes of vibration. Spectrochim. Acta Part A Mol Spectrosc 1972; 28(8): 1485-1496.
https://doi.org/10.1016/0584-8539(72)80118-1

[43] Gall MJ, Hendra PJ, Peacock CJ, Cudby MEA, Willis HA. Laser-Raman spectrum of polyethylene: Part 1. Structure and analysis of the polymer. Polymer (Guildf) 1972; 13(3): 104-108.
https://doi.org/10.1016/S0032-3861(72)80003-X

[44] Snyder RG. Vibrational study of the chain conformation of the liquid n-paraffins and molten polyethylene. J Chem Phys 1967; 47(4): 1316-1360.
https://doi.org/10.1063/1.1712087

[45] Boumdouha N, Safidine Z, Boudiaf A, Djalel Eddine T, Oukara A. Élaboration et caractérisation mécanique des mousses polyuréthanes modifiés. in Fourth International Conference on Energy, Materials, Applied Energetics and Pollution ICEMAEP 2018, Constantine, Algeria: Université Frères Mentouri Constantine 2018; 1:, 136-142.

[46] Suoninen EJ. Optical microscopy. Surf. Charact. A User's Sourceb 2007; pp. 54-56.
https://doi.org/10.1002/9783527612451.ch1

[47] Grandbois A. Chapitre Iii. in Né à Québec, Les Presses de l'Université de Montréal 2018 ; pp. 70-84.

[48] Malíková M, Rychlý J, Matisová-Rychlá L, Csomorová K. Janigová I, Wilde HW. Assessing the progress of degradation in polyurethanes by chemiluminescence. I. Unstabilized polyurethane films. Polym Degrad Stab 2010; 95(12): 2367-2375.
https://doi.org/10.1016/j.polymdegradstab.2010.08.016

[49] Raka L, Bogoeva-Gaceva G, Lu K, Loos J. Characterization of latex-based isotactic polypropylene/clay nanocomposites. Polymer (Guildf) 2009; 50(15): 3739-3746.
https://doi.org/10.1016/j.polymer.2009.05.044

[50] Allen V, Kalivas JH, Rodriguez RG. Post-consumer plastic identification using Raman spectroscopy. Appl Spectrosc 1999; 53(6): 672-681.
https://doi.org/10.1366/0003702991947324

[51] Bentley PA, Hendra PJ. Polarised FT Raman studies of an ultra-high modulus polyethylene rod. Spectrochim. Acta Part A Mol Spectrosc 1995; 51(12): 2125-2131.
https://doi.org/10.1016/0584-8539(95)01513-3

[52] Peskin AV, Winterbourn CC. A microtiter plate assay for superoxide dismutase using a water-soluble tetrazolium salt (WST-1). Clin Chim Acta 2000; 293(1-2): 157-166.
https://doi.org/10.1016/S0009-8981(99)00246-6

[53] Gierlinger N. New insights into plant cell walls by vibrational microspectroscopy. Appl Spectrosc Rev 2018; 53(7): 517-551.
https://doi.org/10.1080/05704928.2017.1363052

[54] Cherukupalli SS, Ogale AA. Online measurements of crystallinity using Raman spectroscopy during blown film extrusion of a linear low-density polyethylene. Polym Eng Sci 2004; 44(8): 1484-1490.
https://doi.org/10.1002/pen.20144